www.czasopisma.pan.pl PAN www.journals.pan.pl

ARCHIVES of FOUNDRY ENGINEERING

DE GRUYTER OPEN

ISSN (2299-2944)
Volume 16
Issue 4/2016

DOI: 10.1515/afe-2016-0103

Published quarterly as the organ of the Foundry Commission of the Polish Academy of Sciences

163 – 168

Microstructure of Cast High-Manganese Steel Containing Titanium

G. Tęcza [a, *], A. Garbacz-Klempka [b]

[a] Department of Cast Alloys and Composites Engineering, Faculty of Foundry Engineering, AGH University of Science and Technology, Reymonta 23 Str., 30-059 Kraków, Poland

[b] Department of Moulding Materials, Mould Technology and Cast Non-Ferrous Metals, Faculty of Foundry Engineering, AGH University of Science and Technology, Reymonta 23 Str., 30-059 Kraków, Poland

*Corresponding author. E-mail address: tecza@agh.edu.pl

Received 16.05.2016; accepted in revised form 12.07.2016

Abstract

Widely used in the power and mining industry, cast Hadfield steel is resistant to wear, but only when operating under impact loads. Components made from this alloy exposed to the effect of abrasion under load-free conditions are known to suffer rapid and premature wear. To increase the abrasion resistance of cast high-manganese steel under the conditions where no dynamic loads are operating, primary titanium carbides are formed in the process of cast steel melting, to obtain in the alloy after solidification and heat treatment, the microstructure composed of very hard primary carbides uniformly distributed in the austenitic matrix of a hardness superior to the hardness of common cast Hadfield steel. Hard titanium carbides ultimately improve the wear resistance of components operating under shear conditions. The measured microhardness of the as-cast matrix in samples tested was observed to increase with the increasing content of titanium and was 380 HV0.02 for the content of 0.4%, 410 HV0.02 for the content of 1.5% and 510 HV0.02 for the content of 2 and 2.5%. After solution heat treatment, the microhardness of the matrix was 460÷480 HV0.02 for melts T2, T3 and T6, and 580 HV0.02 for melt T4, and was higher than the values obtained in common cast Hadfield steel (370 HV0.02 in as-cast state and 340÷370 HV0.02 after solution heat treatment). The measured microhardness of alloyed cementite was 1030÷1270 HV0.02; the microhardness of carbides reached even 2650÷4000 HV0.02.

Keywords: Innovative foundry technologies and materials, Cast high-manganese steel, Primary carbides, Microstructure, Microhardness

1. Introduction

Today, components such as mill lining elements, beaters, jaws and cones of crushers, parts of construction machinery and parts operating in the power industry are manufactured from cast high-manganese Hadfield steel, or alternatively, from its modifications containing the additions of carbide-forming elements, such as chromium and molybdenum. The use of this cast steel grade for the above mentioned components is dictated by the working conditions of castings, which are exposed to the impact of operating loads. When a component cast from Hadfield steel operates under the conditions of mild loads, e.g. sand abrasion, its wear resistance is comparable to that of cast carbon steel [1÷5]. Table 1 shows a variety of the most widely used chemical compositions of cast Hadfield steel, which may contain the following elements (in wt%). In as-cast state, the microstructure of Hadfield steel consists of an austenitic matrix with precipitates of the alloyed cementite $(Fe, Mn)_xC_y$. It may also contain some non-metallic inclusions, and above the phosphorus content of 0.04% [1], also a triple phosphorus-carbide eutectic $(Fe (Fe, Mn)_3 C- (Fe, Mn)_3P)$ [5], (Fig. 1). Carbides precipitating during the solidification and cooling of castings form a network on the austenite grain boundaries, reducing mainly the alloy toughness.

The precipitation of numerous carbides results in the formation of high internal stresses, which may lead to premature failure of castings due to the formation of cracks even at the stage of casting solidification in foundry mould. The low ductility of as-cast components made from Hadfield steel justifies the heat treatment to which these components are subjected and which consists in solutioning and cooling in water. This type of heat treatment allows obtaining the structure based on an austenitic matrix free from the precipitates of alloyed cementite [7÷12] (Fig. 2). Some grades of the cast Hadfield steel are intentionally enriched with small amounts of strong carbide-forming elements, such as chromium or molybdenum. The aim is to improve the abrasive wear resistance of components cast from such alloys. Changes in the chemical composition lead to changes in the microstructure, ultimately resulting in the fact that large amounts of complex carbides precipitate in the casting not only outside but also inside the grain boundaries [7÷12] (Fig. 3). Solutioning of castings made from the alloys with high content of carbide-forming elements does not guarantee obtaining a purely austenitic structure. Unfortunately, neither increase of the austenitizing temperature nor prolongation of its time can offer such a guarantee (Fig. 4) [12].

Table 1.
Examples of the chemical composition of cast high-manganese austenitic steel [1÷12]:

Designation	Chemical composition [wt. %]							
	C	Mn	Si	P	S	Cr	Ni	Mo
GX 120Mn13	0.9÷1.0	11.5÷14	≤1.0	≤0.07	≤0.03	–	–	–
	1.1÷1.3	11.5÷14	≤1.0	≤0.07	≤0.03	–	–	–
	1÷1.4	12÷14	0.3÷1	≤0.10	≤0.03	≤1.0	≤1.0	–
GX 120MnCr13-2	1÷1.4	12÷14	0.3÷1.0	≤0.1	≤0.03	0.6÷1.3	–	–
	1.0÷1.3	11.5÷14	≤1.0	≤0.07	≤0.03	1.5÷2.5	–	–
GX 120MnNi13-3	0.7÷1.3	11.5÷14	≤1.0	≤0.07	≤0.03	–	3÷4	–
GX 120MnMo13-2	0.7÷1.3	11.5÷14	≤1.0	≤0.07	≤0.03	–	–	0.9÷2.1
	1.0÷1.4	11.5÷14	≤1.0	≤0.07	≤0.03	–	–	1.8÷2.1
GX 120MnCr17-2	1.3÷1.5	16.5÷19	0.4÷0.8	≤0.08	≤0.04	2÷3	≤0.60	≤0.50

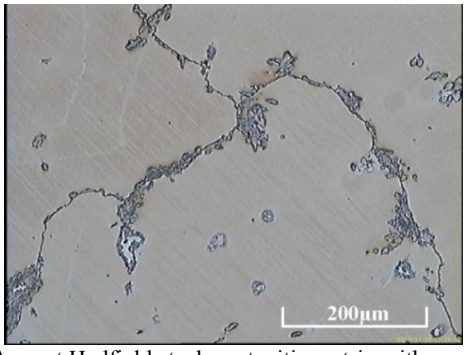

Fig. 1. As-cast Hadfield steel; austenitic matrix with precipitates of alloyed cementite; nital etching [7÷9]

Fig. 2. Cast Hadfield steel after solution heat treatment in water; austenitic matrix free from the precipitates of alloyed cementite; nital etching [7÷9]

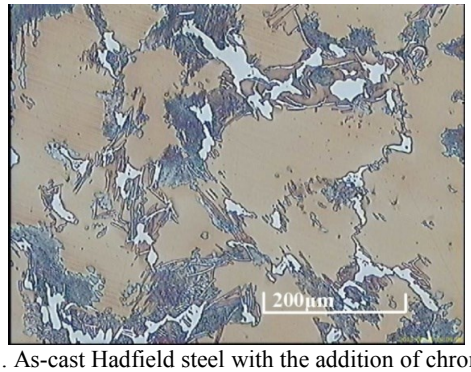

Fig. 3. As-cast Hadfield steel with the addition of chromium (Cr 1.4%); austenitic matrix with numerous precipitates of alloyed cementite; nital etching [12]

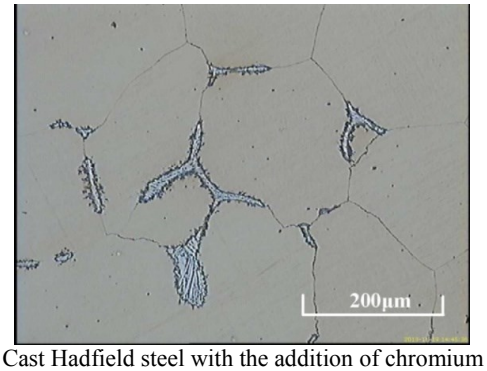

Fig. 4. Cast Hadfield steel with the addition of chromium (1.4% Cr) after solution heat treatment in water; austenitic matrix with undissolved carbides distributed on grain boundaries; nital etching [12]

It is known from the technical literature [6] that the composition of cast high-manganese steel can be enriched with additions of vanadium. At a level of 2.3% C, 11% Mn and about 6% V, the resulting structure consists of an austenitic matrix with eutectic vanadium carbides (Fig. 5). Carbides of this type present in the test melts were reported to cause very low impact strength (of the order of 3÷6 J/cm^2). In another case described in [11], with the content of 1.6% C, 10% Mn, 5.5% V, the authors obtained the microstructure consisting of an austenitic matrix with primary carbides uniformly distributed in this matrix (Fig. 6). In the abrasion test using Miller machine, this cast steel showed two times higher resistance than the common cast Hadfield steel [11]. Very positive results following the introduction of vanadium to the alloy have encouraged the author to make further test melts of the high-manganese steel, this time with the addition of titanium, which in the presence of carbon forms carbides of even higher hardness.

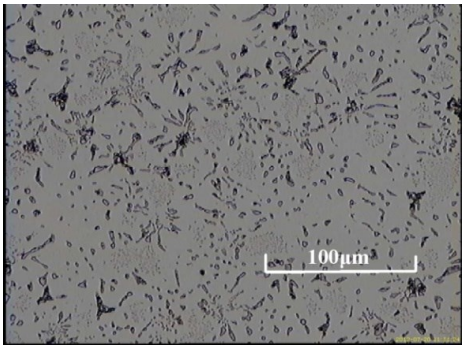

Fig. 5. Cast high-manganese steel containing 2.3% C, 11% Mn and 6%V; austenitic matrix with precipitates of eutectic vanadium carbides; nital etching [6]

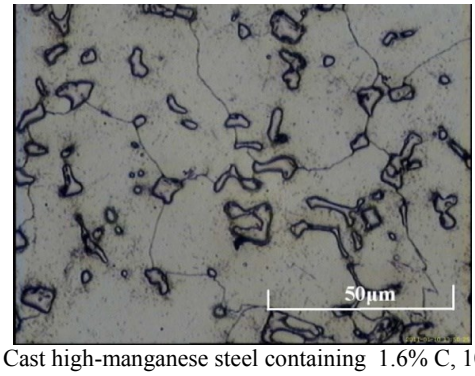

Fig. 6. Cast high-manganese steel containing 1.6% C, 10% Mn and 5.5% V; austenitic matrix with uniformly distributed primary carbides; nital etching [11,13]

2. Test materials and methods

Samples were cut out from the Y type ingots cast from high-manganese steel melted in an induction furnace of 30 kg capacity from Hadfield steel scrap with the additions of Fe-Ti. Introducing appropriate amount of titanium to molten steel in a metallurgical process resulted in the formation of primary titanium carbides, which in the solidified steel were evenly distributed in alloy matrix. Four test ingots were cast with different content of carbon and titanium. Samples were taken from the casting with 25 mm wall thickness; some samples were used in as-cast state, other samples were subjected to a solution heat treatment (1050ºC/water). On thus obtained samples, the analysis of chemical composition was conducted using ED/XRF spectrometer, the resulting microstructures were examined under a Neophot 32 light microscope equipped with a camera for digital image recording; microhardness of the matrix and carbides was measured by Vickers method under a load of 20 g. Analysis of the chemical composition of visible precipitates was made under the scanning electron microscope equipped with EDS analyzer.

3. Discussion of results

Based on the results of chemical analysis set out in Table 2, it was found that the content of basic elements in the melt was comparable to the content of these elements in cast Hadfield steel. In test castings, higher content of chromium (1.2÷1.4%) and silicon (1.5÷2.4%) was obtained at a variable titanium content of 0.4÷2.5%.

Table 2.
Chemical composition of the cast high-manganese steel melt

Designation	Chemical composition [wt. %]							
	C	Mn	Si	P	S	Cr	Ni	Ti
T2	1.2	15	1.5	0.04	0.02	1.4	0.1	2.5
T3	0.8	16	2.3	0.04	0.03	1.4	0.2	2.0
T4	1.2	13	2.4	0.03	0.02	0.2	0.1	1.5
T6	1.4	14	1.5	0.07	0.003	1.2	0.2	0.4

Based on the examinations by light microscopy (Figs. 7-13) and SEM (Fig. 14), and on the results of the chemical analysis of visible precipitates (Table 3, Figs. 15-16), it was found that as-cast microstructure of the examined steel is composed of a high-manganese austenitic matrix and primary titanium carbides, evenly distributed in this matrix. In melts T2 and T3, very small quantities of alloyed cementite were observed on grain boundaries (Figs. 7-8). In melts T4 and T6, the amount of the precipitated cementite was significantly higher (Figs. 9-10). The presence of the secondary alloyed cementite precipitated in test melts was due to the high content of chromium, to the presence of titanium (the higher is the content of titanium, the less of cementite is precipitated), and to the heavy segregation of alloying elements during the solidification and cooling of ingots.

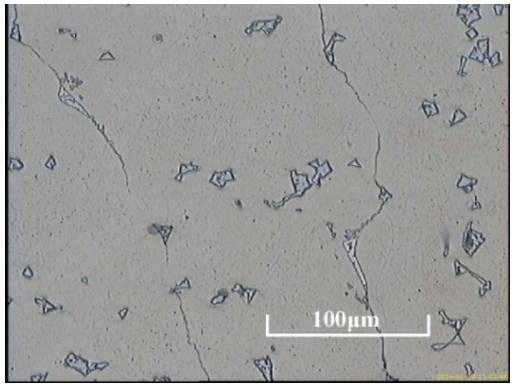

Fig. 7. As-cast microstructure of sample from melt T2; austenitic matrix with evenly distributed primary titanium carbides, alloyed cementite present on grain boundaries; nital etching

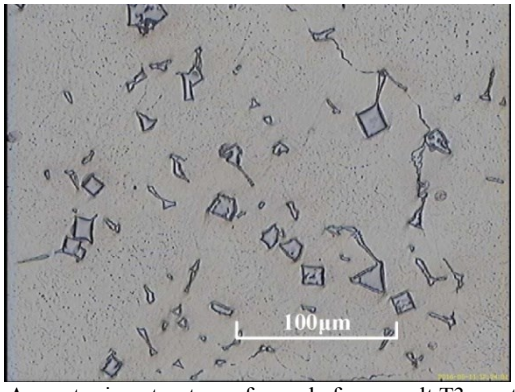

Fig. 8. As-cast microstructure of sample from melt T3; austenitic matrix with evenly distributed primary titanium carbides, alloyed cementite present on grain boundaries; nital etching

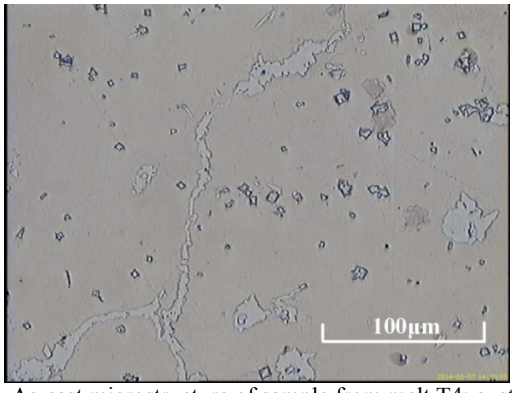

Fig. 9. As-cast microstructure of sample from melt T4; austenitic matrix with evenly distributed primary titanium carbides, alloyed cementite present on grain boundaries; nital etching

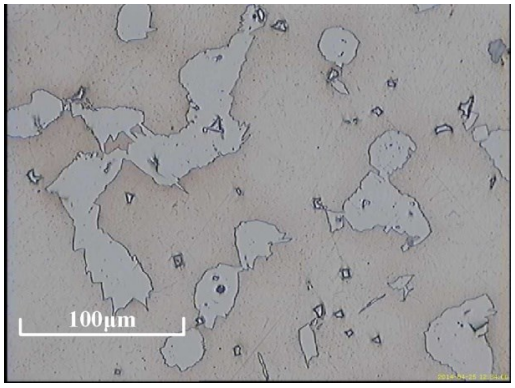

Fig. 10. As-cast microstructure of sample from melt T6; austenitic matrix with evenly distributed primary titanium carbides, alloyed cementite present on grain boundaries; nital etching

Fig. 11. Microstructure of sample from melt T3 after solution heat treatment; austenitic matrix with evenly distributed primary titanium carbides; nital etching

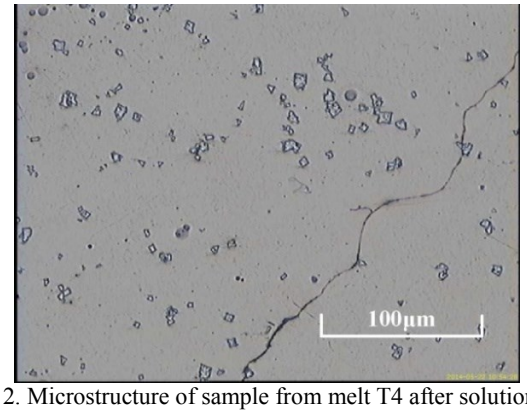

Fig. 12. Microstructure of sample from melt T4 after solution heat treatment; austenitic matrix with evenly distributed primary titanium carbides; nital etching

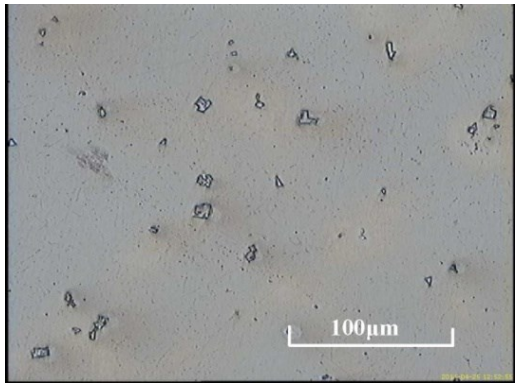

Fig. 13. Microstructure of sample from melt T6 after solution heat treatment; austenitic matrix with evenly distributed primary titanium carbides; nital etching

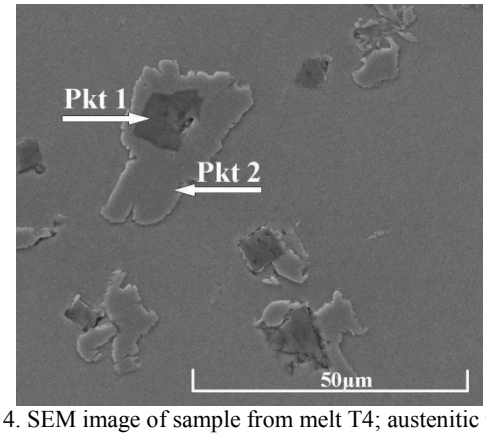

Fig. 14. SEM image of sample from melt T4; austenitic matrix with primary titanium carbides and alloyed cementite present on grain boundaries; nital etching

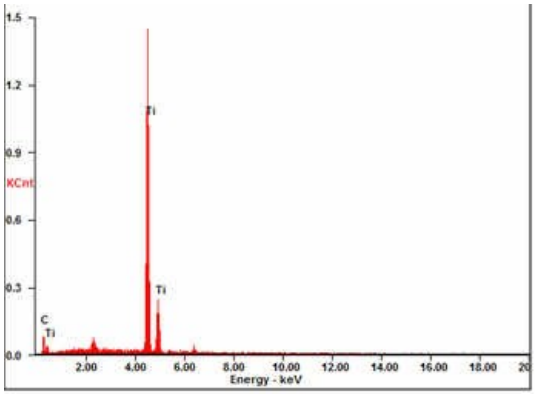

Fig. 15. EDS spectra of visible precipitates of titanium carbide (Pt 1, Fig. 14)

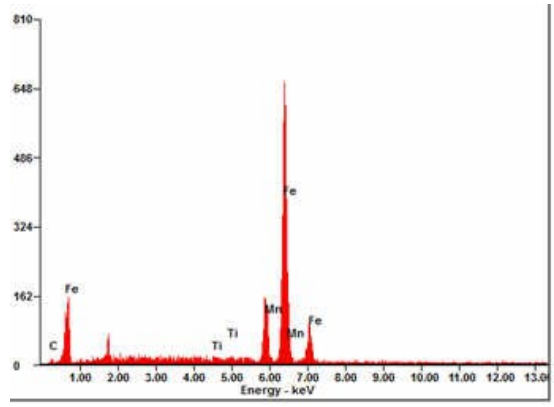

Fig. 16. EDS spectra of visible precipitates of alloyed cementite (Pt 2, Fig. 14)

Table 3.
Example of the chemical composition of visible precipitates

	Pt 1 in Fig. 14	Pt 2 in Fig. 14
	[wt. %]	
C	16.0	3.5
Ti	84.0	1.0
Mn	-	19.0
Fe	-	76.5

The solution heat treatment of test samples changes the microstructure, and consequently in all the tested samples it was possible to obtain the structure composed of an austenitic matrix and primary titanium carbides evenly distributed in this matrix, with grain boundaries free from the presence of cementite precipitates (Fig. 9).

The measured microhardness of the as-cast matrix in samples tested was observed to increase with the increasing content of titanium and was 380 HV0.02 for the content of 0.4%, 410 HV0.02 for the content of 1.5% and 510 HV0.02 for the content of 2 and 2.5%. After solution heat treatment, the microhardness of the matrix was 460÷480 HV0.02 for melts T2, T3 and T6, and 580 HV0.02 for melt T4, and was higher than the values obtained in common cast Hadfield steel (370 HV0.02 in as-cast state and 340÷370 HV0.02 after solution heat treatment).

The measured microhardness of alloyed cementite was 1030÷1270 HV0.02; the microhardness of carbides reached even 2650÷4000 HV0.02.

4. Conclusions

1. As-cast microstructure of the tested steel consists of a high-manganese austenitic matrix, primary titanium carbides uniformly distributed in this matrix, and alloyed cementite.
2. After solution heat treatment, the obtained structure consists of an austenitic matrix and primary titanium carbides evenly distributed in this matrix.
3. As-cast microhardness of the alloy matrix is 380÷510 HV0.02 and increases with the increasing titanium content.
4. Solution heat treatment leads to further increase of the matrix microhardness (up to 580 HV0.02).

5. Microhardness of the alloyed cementite and carbides reaches 1270 HV0.02 and 4000 HV0.02, respectively.

References

[1] Kniaginin, G. (1968). *Austenitic manganese cast steel*. Kraków: PWN. (in Polish).

[2] Smith, R.W., DeMonte, A. & Mackay W.B.F. (2004). Development of high-manganese steels for heavy duty cast-to-shape applications. *Journal of Materials Processing Technology*. 153-154, 589-595.

[3] Głownia, J. (2002). *Castings alloy steel - application*. Kraków: Fotobit. (in Polish).

[4] Głownia, J., Kalandyk, B., Furgał, G. (1999). *Characteristics of cast steel alloy*. Kraków: Wyd. AGH, Skrypt SU1569. (in Polish).

[5] Telejko, I. (2004). *The fragility of the steel in the temperature range of the solid-liquid.* Kraków: Wyd. Naukowe Akapit. (in Polish).

[6] Krawiarz, J. & Magalas, L. (2005). Hadfield modified cast steel with increased resistance to abrasion. *Przegląd Odlewnictwa.* 10, 666-672. (in Polish).

[7] Tęcza, G., Głownia, J. & Rąpała, M. (2008). The phenomenon of segregation in thick-walled castings with cast Hadfield, *Przegląd Odlewnictwa*. 1-2, 10-15. (in Polish).

[8] Sobula, S. & Tęcza, G. (2009). Hadfield steel microstructure stabilization at elevated temperature in the presence of chromium. *Przegląd Odlewnictwa*. 3, 132-137. (in Polish).

[9] Sobula, S., Tęcza, G., Rąpała, M., Stańczak, S. & Głownia, J. (2008). The effects of supersaturating cast Hadfield in polymers. *Przegląd Odlewnictwa*. 7-8, 378-382. (in Polish).

[10] Kalandyk, B. & Zapała, R. (2013). Effect of high-manganese cast steel strain hardening on the abrasion wear resistance in a mixture of SiC and water. *Archives of Foundry Engineering*. 13(4), 63-66.

[11] Głownia, J., Asłanowicz, M. & Ościłowski, A. (2013). Tools cast from the steel of composite structure. *Archives of Metallurgy and Materials*. 58(3), 803-808.

[12] Tęcza, G. & Sobula, S. (2014). Effect of heat treatment on change microstructure of cast high-manganese hadfield steel with elevated chromium content. *Archives of Foundry Engineering*. 14(3), 67-70.

[13] Tęcza, G. & Głownia, J. (2015). Resistance to abrasive wear and volume fraction of carbides in cast high-manganese austenitic steel with composite structure. *Archives of Foundry Engineering*. 15(4), 129-133.